This is the author's version of an article that has been published in the IECON 2021 proceedings.
Changes were made to this version by the publisher prior to publication.
The final version of record is available at https://dx.doi.org/10.1109/IECON48115.2021.9589196

Three-Layer Hierarchical Model Predictive Control Concept for Industrial DC Microgrids

Elias Knöchelmann*, Alexander Männel† and Moritz Schappler*
*Gottfried Wilhelm Leibniz Universität Hannover, Institute of Mechatronic Systems, Hannover, Germany
Email: Elias.Knoechelmann@imes.uni-hannover.de
†Bosch Rexroth AG, Lohr am Main, Germany

***Abstract*—This paper presents an extension of the dual-layer model predictive control (MPC) for industrial DC microgrids. This structure allows an easier integration of stochastic methods on all levels. Moreover, in the new three-layer MPC, energy storages are proposed for each level. As a proof of concept, a control is presented for the new layer, the primary control level in microgrids. The MPC as a central control strategy, has the disadvantage that a new model has to be created for new bus participants. By a simply expandable state space model and a parameterization with data sheet values, this disadvantage can be refuted. Further, for the application on a programmable logic controller (PLC), a simpler and faster MPC with an equal control performance, is presented.**

***Index Terms*—MPC, DC Microgrid, Three-Layer MPC Control**

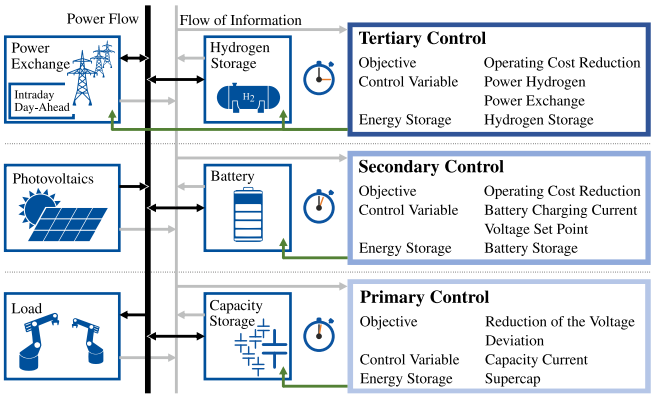

Fig. 1. Proposed control structure for DC MGs.

I. Introduction

Small manufacturing companies often have great difficulties to withstand the price pressure against larger companies. Especially since, unlike large companies, they are not excluded from many taxes (at least in Germany), like the tax on electricity. It can be worthwhile for such companies to integrate renewable energy as a decentralized supplier, to lower production costs. To take into account the volatility of renewable energies, energy storage systems (ESS) can be used. Those small sub grids with decentralized suppliers and storage devices are called microgrid (MG). The ESS and as well as regenerative energy are easier to connect to direct current (DC) MG, since batteries work with DC [1]. DC systems have further advantages, e.g. inverters of electric motors can distribute braking energy directly via the DC grid, converter losses are reduced, space requirements are reduced by replacing decentralized rectifiers with one central supplier and the modeling is simpler. Especially for small companies in the price competition, a DC MG with decentralized renewable energies can be an alternative, because MG not only allow consumers to determine the time to sell or buy energy, but also how they deal with renewable energy [2]. Components are available, but there is still a need for research in the area of grid control. The aim of this paper is to present a uniform MPC concept, based on cascade control for industrial DC MG, so that safe operation can be guaranteed, as well as to reduce the operating costs of its user. The concept is shown in Fig. 1 and is based on the hierarchical rule structure of [3].

MPC-based control are already present at all levels [4], therefore, a unified concept of MPC is reasonable.

MPC have the disadvantage that they are central controls, require a system model, and an optimization problem must be solved in real time. However, at the tertiary level, these disadvantages, except for run time, no longer come into play. Thus, in [5] MPC, rule based control (RBC), and stochastic model predictive control (SMPC) were compared for a MG, with the MPC variants being much more efficient. In [6], an islanded MG was studied. It was shown that an SMPC could reduce the use of fossil fuels. Bordons et al. show in their book [7] their summarized research results in MPC for MG, but without primary control. In the MPC in primary control uses different principals than in the other levels [4].

In summary, especially at the tertiary level many MPC variants are used. In [8], a two-layer SMPC scheme was presented, but this does not involve the primary level. Moreover, in this concept, the inner MPC is without stochastic part. In this publication, this concept is extended to all three levels (see [3]) and a suitable energy storage combination is proposed, see Fig. 1. Different MPC variants for the tertiary and secondary levels have already been presented [8], so for the proof of concept, we present only a simple MPC for the primary level. The primary control in the literature focuses on decentralized control of converters i. e. replacement of the droop control [9], [10]. In this paper also the droop control is replaced, but the current controller of the inverter is still used. In addition,

the proposed central controller has many more states than controllers in the literature [9].

In order to counteract the mentioned disadvantages of MPC-procedures in the field of MG control, an easily extendable model, parameterizable by data sheets, is created. Together with the assumption that the considered MGs are for small factories and changes to the electrical distribution are relatively rare, the disadvantages of a model-based procedure can be invalidated. The major problem with centralized control is the dependence on the main controller, which can be mitigated by decentralized contingency characteristics in case of communication failure. Solving an optimization problem on the other hand is more difficult on the PLC due to its computing architecture. Therefore, the standard MPC is compared with a fast and less complex discrete model predictive trajectory set control (MPTSC) [11].

The main contributions of this paper are

- the proposition of an MPC cascade structure, which is specially adapted for industrial MGs,
- a simple and easily extensible DC MG dynamic system model,
- a comparison between a normal MPC and an MPC with discrete values.

The remainder of the paper is structured as follows: Sec. 2 presents in detail the proposed MPC cascade structure. The system model required for MPC is introduced in Sec. 3. This is then used in the two MPC variants introduced in Sec. 4. To compare the MPCs, an experimental setup is introduced in Sec. 5. Based on this, the results are presented in Sec. 6 and the conclusion in Sec. 7.

II. Control structure concept

The proposed concept is aimed at small companies with the goal of introducing renewable energy and (thereby) reducing operating costs resulting from high electricity costs. A special aspect is that dynamic loads are taken into account. Thus, the concept is particularly well suited for small robot- or machine tool-intensive production.

In the state of the art the hierarchical rule structure of [3] has become generally accepted. This concept is maintained and extended for connection to the electricity market. Since participation in the electricity market requires a constant demand over a certain horizon, we suggest an energy storage system for each cascaded control level. This balances power peaks and dips, generated by the uncertain renewable energy source. The complete structure is shown in Fig. 1

The goal of any power grid is to supply consumers with electric energy. In addition, the operating costs of the MG should be reduced for the operators. This shall be done by the consequent use of SMPC processes which can incorporate uncertainties into the load prediction, thus increasing reliability and/or cost savings. However, it is still possible to incorporate simpler standard MG control procedures into the proposed structure.

To simplify the nomenclature, the level of the control is written in parentheses before the control. For example, the (P)MPC is the model-based predictive control of the primary level. Each level is discussed in detail in the following sections.

A. Primary Control

The task of the primary level is to supply load (in our case robots) with sufficient electrical power and to maintain the voltage level. The control of the current is carried out decentrally directly on the inverters and controls in sync with the switching cycle of the inverter. The control cycle frequency for the voltage control is chosen around 50-100 Hz to be in range of the highly dynamic loads. Another characteristic of robots and other mechatronic systems is that their power consumption varies strongly (see Fig. 4). This requires an energy storage which has a fast response, a high power density and also a high cycle life. Thus, a capacitive storage system is the obvious choice.

The main goal of the control is to supply all loads with electric energy. The secondary goal is to have enough storage reserves for an extreme situation (e.g. extreme power deficit/surplus). A possible tracking cost function J at time step k for the MPC would be

$$\begin{aligned} J = &\sum_{i=1}^{N_\mathrm{p}} \left\| \boldsymbol{Q} \left(\boldsymbol{y}(k+i) - \boldsymbol{y}_\mathrm{R}(k+i) \right) \right\|^2 + \\ r_1 \cdot &\sum_{i=1}^{N_\mathrm{p}} \left\| \boldsymbol{u}(k+i-1) \right\|^2 + r_2 \cdot \sum_{i=1}^{N_\mathrm{c}} \left\| \Delta \boldsymbol{u}(k+i) \right\|^2, \end{aligned} \tag{1}$$

where N_p is the prediction horizon and N_c is the manipulated variable horizon; $\boldsymbol{Q}$, r_1 and r_2 are weighting matrices, $\boldsymbol{y}$ is the output variable and $\boldsymbol{u}$ is the manipulated variable.

In addition, there is the requirement from the stock market that the power demand must remain constant. The power consumption of the robots is particularly subject to uncertainties. Including these uncertainties can reduce voltage cap violations or improve supply reliability by scheduling larger reserves. The particular challenge in this area is the fast cycle time, which could be too short for scenario-based approaches for MPC. On the other hand, analytical approaches also have major runtime problems on typical industrial hardware for this level of control.

B. Secondary Control

At this level, the aim is to ensure that the capacity level is always sufficient to supply the robots. As a secondary objective, line losses and the operating costs of the battery are to be minimized. The control cycle in this level is based on the renewable energies and the energy storage and should be approx. 1–10 s. In this level, response time and high cycle life are not as important as in the primary level. However, since high energy density is needed, we propose to use a lithium-ion battery.

Also in this level, there must be no trading with the power exchange, so there must be enough energy in the battery to bridge extreme cases (grid downtimes, weather fluctuations [12]). Stochastic disturbance variables are mainly the renewable energy yield and production adjustments.

This is the author's version of an article that has been published in the IECON 2021 proceedings.
Changes were made to this version by the publisher prior to publication.
The final version of record is available at https://dx.doi.org/10.1109/IECON48115.2021.9589196

Since the goal in this level is to achieve a reduction in operating costs in addition to balancing energy shortages by the battery, we propose an economic model predictive control. A possible cost function J could include:

$$J = \sum_{i=1}^{N_\mathrm{p}} C_\mathrm{loss}\left(k+i\right) + \sum_{i=1}^{N_\mathrm{p}} C_\mathrm{bat}\left(k+i\right) + a \cdot \left\| S_\mathrm{SC}\left(k+n\right) - S_\mathrm{SC,setp} \right\|^2 . \tag{2}$$

The loss cost C_loss is the transmission loss multiplied by the electrical power cost. The scaling factor a can be used to set the significance so that the state of charge (SoC) of the supercapacity S_SC is close to the nominal value $S_\mathrm{SC,setp}$.

Especially the inclusion of the battery lifetime according to [13] in the cost function as batterycost C_bat has the disadvantage that it is then no longer linear and thus cannot be reliably solved in small time. Since solving a non-convex problem takes much more time, time is also a major issue here, especially with the stochastic reformulations.

C. Tertiary Control

In this level it is possible to reduce operating costs by interacting with the power exchange through advantageous trade deals. This means that the economic aspect has a much greater influence on operating behavior at this level, since security of supply can almost always be ensured by purchasing power.

The power exchange results in many constraints [7], since trading is only allowed at certain times. In addition, bids must sometimes be completed up to 36 h before the power is delivered. This requires good predictions and a long prediction horizon. The regular cycle is also specified by the power exchange to 15 min. A long-term energy storage is needed to cope with power outages, to use only self-generated electricity or to generate trading profits in the electricity market. Hydrogen storage is a possible long-term storage solution.

Uncertainties in this level are again the weather, since predictions are made over a very long horizon. Deviations between predicted and actual energy lead to power differences which have to be absorbed by energy storage. In addition the change in the electricity price cannot be predicted exactly.

The goal here is therefore clearly to reduce operating costs by taking advantage of electricity trading C_trade, the hydrogen storage C_hyd, the battery storage C_bat and renewable energies. The cost function J could result to

$$J = \sum_{i=1}^{N_\mathrm{p}} \left(C_\mathrm{trade}\left(k+i\right) + C_\mathrm{bat}\left(k+i\right) + C_\mathrm{hyd}\left(k+i\right) \right). \tag{3}$$

Problematic are the many constraints resulting from the electricity market (e.g. discrete trading volumes, fixed trading hours, no guaranteed trading conclusion in the spot market, etc.), the long prediction horizon and the large number of uncertain variables (load demand, renewable energies, spot market, etc.).

III. Control-Oriented Model

To allow a real-time implementation, a model with low computational requirements and therefore reduced complexity is required. In addition, the model should be easy to expand for new bus participants. Therefore all loads and sources are represented by a real power source. The main reason for this is that the inverters internally have an essential fast current control and so the current can be given by the MPC. Electric lines are modeled using the π circuit diagram and the DC link capacitance is modeled as such. The components are shown in Fig. 2.

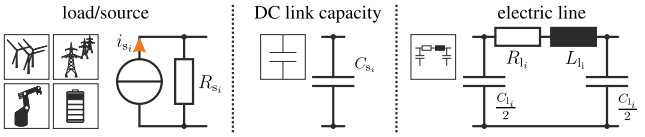

Fig. 2. Composition of the modeling modules for all loads and suppliers.

These models can now be parameterized via cable manufacturer standards [14] and inverter manuals [15]. Since the inductance of the line is very small and its time constant is far below the sampling frequency, it can be neglected, c. f. [16]. Cable capacitance could also be removed in this way, but these do not affect modeling complexity, so they are retained. The components are now joined together to create a module for each power supply participant. The equivalent circuit diagram for one producer and one consumer is shown in Fig. 3.

All components were approximated by a real current source i_s, since this is the internal controlled variable of the active components (ESS, active front end (AFE)). This current i_s is also the input u of the state-space model (Eqn. 1). The intermediate circuit capacitors C_s were connected in parallel to a real current source. The wires were simulated via the π equivalent circuit.

One half of the line capacitance C_l is parallel to the intermediate circuit capacitance C_s and these were therefore summed up. The voltage u_{C_i} of this capacitance i is also the state $\boldsymbol{x}$ and output $\boldsymbol{y}$ of the state-space model. The line resistance R_l connects this capacitance to the final capacitance. This consists of the sum of all line end capacitances and simultaneously describes the voltage of the DC bus u_{C_n}. The current source, DC link capacitance and cable, without the end capacitance, constitute as a module. The linear state space representation of this module i results to:

$$\begin{aligned} \dot{\boldsymbol{x}}(t) &= \boldsymbol{A}\boldsymbol{x}(t) + \boldsymbol{B}\boldsymbol{u}(t), \quad \boldsymbol{x}(0) = \boldsymbol{x}_0, \\ \boldsymbol{y}(t) &= \boldsymbol{C}\boldsymbol{x}(t) + \boldsymbol{D}\boldsymbol{u}(t), \\ x = y &= u_{\mathrm{C}_i}, \quad a = -\frac{R_{\mathrm{s}_i} + R_{\mathrm{l}_i}}{R_{\mathrm{s}_i} R_{\mathrm{l}_i} \left(C_{\mathrm{s}_1} + \frac{C_{\mathrm{l}_1}}{2} \right)}, \\ b &= \frac{1}{C_{\mathrm{s}_1} + \frac{C_{\mathrm{l}_1}}{2}}, \quad c = 1, \quad d = 0. \end{aligned} \tag{4}$$

The modules can now be coupled with the Compositional Modeling to the coupling block's final capacitance. Thus any

This is the author's version of an article that has been published in the IECON 2021 proceedings.
Changes were made to this version by the publisher prior to publication.
The final version of record is available at https://dx.doi.org/10.1109/IECON48115.2021.9589196

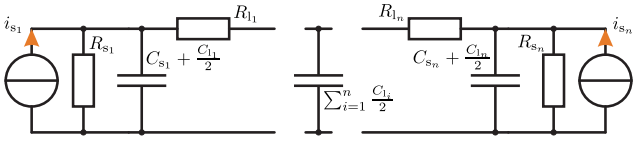

Fig. 3. Schematic structure of the physical model of two components with the coupling capacity.

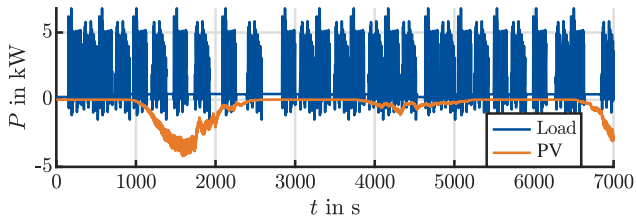

Fig. 4. Power curves of the robots (blue) and the PV (orange), which were used to test the control structure.

number of modules can be connected and the model can be extended with new components.

For each ESS an additional state for the SoC must be defined. However, more accurate storage models from the literature can also be used. The SoC was read from the battery management system. The power source i_{sBat} becomes then a controlled power source, which is controlled by the storage management system.

IV. Primary Level MPC – (P)MPC

Model-based control methods are mainly used in slow processes [17]. This is due to the functional principle of the MPC. Based on a system model, the best possible manipulated variable sequence $\boldsymbol{u}$ is determined in order to minimize a cost function J:

$$\min_{\boldsymbol{u}} J(\boldsymbol{x}, \boldsymbol{u}) = V\left(\boldsymbol{x}\left(N_{\mathrm{P}}\right)\right) + \sum_{k=1}^{N_{\mathrm{P}}} l\left(\boldsymbol{x}_k, \boldsymbol{u}_k\right) \tag{5}$$

$$\begin{aligned} \text{s.t.:} \quad & \boldsymbol{x}_{k+1} = \boldsymbol{f}(\boldsymbol{x}, \boldsymbol{u}) \\ & \boldsymbol{u}_k \in \mathcal{U} \quad \forall k = 1, \ldots, N_{\mathrm{U}} \\ & \boldsymbol{x}_k \in \mathcal{X} \quad \forall k = 1, \ldots, N_{\mathrm{P}} \end{aligned}$$

The cost function $\boldsymbol{J}$ is divided here into terminal costs V, which evaluate the costs of the system trajectory at the end of the prediction horizon N_{P}, and integral costs l, which evaluate the costs along the prediction horizon. The sequence of manipulated variables is chosen from the range of admissible manipulated variables $\mathcal{U}$ considering the admissible states $\mathcal{X}$. Thus, constraints are directly taken into account. The solution of the optimization is thus an optimal sequence of manipulated variables, of which the first manipulated variable is used as system input. In the next step $k+1$ the optimization problem (OP) is solved again with (in our case) newly measured states.

A. Model Predictive Trajectory Set Control (MPTSC)

In a linear state space model, a convex optimization problem must be solved for the optimal manipulated variable. On industry-typical PLCs, this is often a problem at fast control rates. To solve this problem, following [11] a discrete control set

$$\boldsymbol{u}^* := \{u^*_{\min}, u^*_{\min} + \Delta u^*, u^*_{\min} + 2\Delta u^* \ldots u^*_{\max}\} \in \mathcal{U} \tag{6}$$

is used. Then, from this set $\boldsymbol{u}^*$, the (sub)optimal solution for cost function J is selected, c. f. [11].

The disadvantage of this method is that there is no optimal solution and the manipulated variable jumps at every change. With MPC, on the other hand, the ratio of actuator activity and control deviation can be set via two matrices. Since the actuator is an electrical converter, which sets the output via a pulse width modulation (PWM), actuating activity (also jumps) is irrelevant. The aspect of the (sub) optimal solution is discussed in more detail in the next chapter.

V. Test Setup

To show the suitability of the concept, the (P)MPC is implemented at an exemplary test facility. This facility consists of an AFE as load, an AFE as supply, and an ESS with DC-DC converter.

As ESS a lithium-ion battery was available. A use of this ESS in the primary level would be, due to the short charge and discharge cycles, bad for the life span. Therefore in this paper the AFE is used instead of the capacity storage in the real implementation. Thus, at least in the simulation, the conceptual constraints were also tested. The difference between the use of the AFE and the supercapacity model is mainly a simplification of the model (no efficiency and state of charge required) and a simplification of the constraints. Assuming that the supercapacity model is improved by a feedback of measurements, we assume that a simulation is sufficient for the validation of the constraints (at least for the primary level).

The supply AFE [15] has a nominal power of 140 kW and is therefore designed for larger loads. The switching frequency of the AFE is 4 kHz, so rather slow compare to smaller devices, to reduce switching losses. One effect of this low switching frequency is that the control in particular reacts slowly to changes and thus the voltage has a large control error. This can also be seen in the unloaded case, where the voltage scatters about ± 5 V (see the first 170 s in Fig. 6), so the manipulated variable has a great uncertainty. For this reason, the suboptimal control solution, doesn't have an extremely negative influence, since the required manipulated variable cannot be set perfectly. The internal current control of the AFE is with 4 kHz control clock much faster than the (P)MPC (100 Hz).

As load, a randomized data set (see Fig. 4) was generated for each robot covering twice 50 point to point movements. The power curves of these four robots were merged together with different pause lengths. The data for the photovoltaic system are measurements originated from a domestic facility. To increase the variance in the data, measurements were scaled down from 2.5 days to 2 hours. This also has the effect that a more complex test scenario has been created.

A detailed description of the test setup can be found in [18].

A. Model validation

To validate the model, presented in chapter 3, which is used for prediction in the MPC the described experimental setup with a voltage droop curve as control, is used. Since the model is used in the MPC and data sheet values are used, it should be checked in advance how well the system is represented. The comparison of the simulated AFE voltage (first model state) and the real AFE voltage is shown in Fig. 5.

The voltage curve of the first state matches the measurement well. However, it is noticeable that the voltage measurement is very noisy. This is mainly due to the low switching frequency of the AFE of 4 kHz which results in a root mean square error (RMSE) of 2.5 V. This roughly corresponds to the measurement noise. However, the power curve has large deviations in the first 20 s, the power RMSE is 57 W here. The non-linear component effects (saturation, temperature dependency etc.) of the AFE are visible, which were neglected in the modelling. To improve the modeling result, all model parameters could still be identified or a more complex model could be used. However, both have the disadvantage that a higher operator overhead is required and thus will not be considered further for the time being.

VI. Results

The MPC and the MPTSC are compared based on runtime and control accuracy. The setpoint for all states was set to 650 V. For the MPC a model with four states (AFE, ESS, load, DC bus) was created. The voltage of the AFE of the described setup with the MPC using a control horizon of three and a prediction horizon of five, is displayed in Fig. 6.

The weighting matrices for actuator activity and control deviation were designed empirically. The voltage curve from Fig. 6 appears very noisy. This is due to the slow PWM frequency, which results in lower switching losses, but also a higher voltage ripple. The voltage ripple with a constant load, i.e. the first 120 s, is ±5 V. This corresponds to the value in Fig. 5, because also here the voltage ripple is ±5 V with constant load (0 to 5 s). At 180 s a strongly changing load (robot movements) starts. From 180 s on the deviation from the nominal voltage increases. The cause for that is,

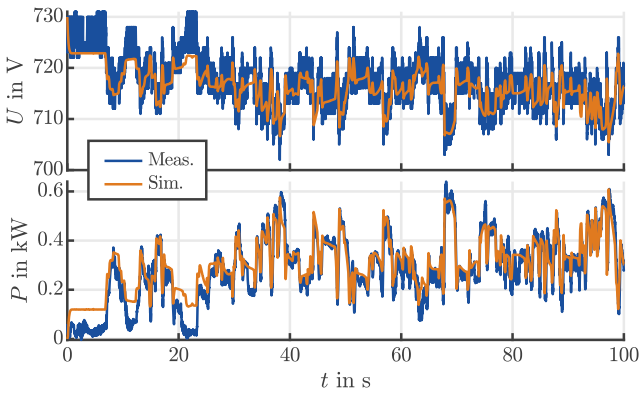

Fig. 5. Comparison of the proposed model with a measurement of the test setup.

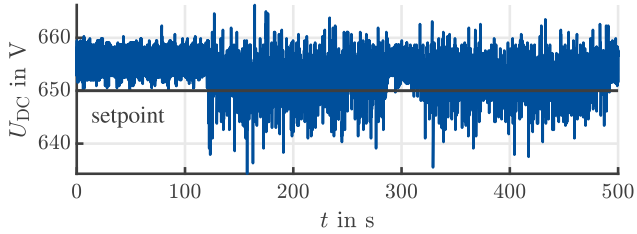

Fig. 6. DC voltage of the AFE capacitance (first state of the model) by using the MPC as voltage control.

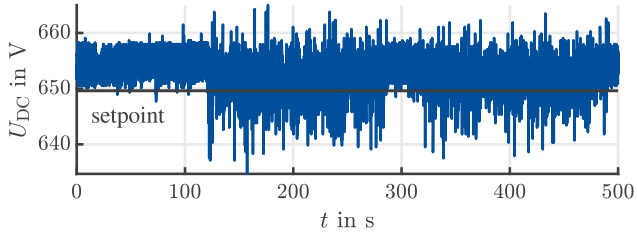

Fig. 7. DC voltage of the AFE capacitance (first state of the model) by using the MPTSC as voltage control.

that the model parameters only originate from a data sheet and were not directly identified at the test facility. This has the advantage that models can be easily constructed, since the identification of model parameters is a dedicated field of research. The drawback are larger control errors result from these model deviations. These control errors can be detected from 180 s onwards. Compared to the control deviation in Fig. 5 (first 5 s in idle mode) this value is smaller. An automatic identification of the model parameters can still lead here to a large improvement of the control error.

The major challenge with the MPC is that the real-time capability suffers with larger electric networks, which produce larger optimization problems. Therefore, the MPTSC presented by [11] was also implemented. This MPC does not solve a continuous optimization problem, but selects the best possible manipulated variable from a predefined set. If the discretization of the manipulated variable is chosen so that it lies below the noise of the manipulated variable, it makes no difference whether a suboptimal solution or an optimal solution is used, since only a suboptimal value is set anyway. The MPTSC was tested on the test setup with the same parameters and an output set from -15 to 15 A in 1 A steps. The results are shown in Fig. 7. As predicted, a direct comparison of the voltage shows no difference between the MPC and the MPTSC.

Fig. 7 and Fig. 6 represent only the first 15 min of the test scenario. Table I therefore shows the mean and standard deviation of the control variable for 2 h. Here it can even be seen that the MPTSC not only does not deposit worse, but also better than the MPC. This is mainly due to the unidentified model. Especially with the parameterization by data sheet values, many other effects are neglected, which are otherwise considered in the identified parameters.

To compare only the runtimes of the control processes, the algorithm was simulated on a PLC. Especially for the

	AFE Voltage	
	mean	σ
MPC with 4 States	652.8 V	3.1 V
MPTSC with 4 States	652.3 V	3.0 V

TABLE I
COMPARISON OF CONTROL ACCURACY OF MPC AND MPTSC.

communication and the load calculation (c. f. [18]) a larger overhead is needed. Thus, only the algorithms are compared in the runtime comparison. To show that MPTSC can also control larger networks in a satisfactory time, a model with eight states (AFE, ESS, Photovoltaics (PV), four times load, DC bus) was also created for the runtime comparison. The results are shown in Fig. 8 and Table II. It can be seen that the MPTSC with four states is nine times faster than the normal MPC with four states, and 17 times faster with 8 states. This difference thus only increases with increasing number of states and prediction horizon length. This is due to the fact that no matrix inverse has to be solved for MPTSC. Thus the algorithmic complexity (in O notation) of the MPC is $O(n^3)$ (because of the matrix inverse) and that of the MPTSC $O(n^2)$, where n depends on the number of states and the prediction horizon. For PLCs there are linear algebra toolboxes, but fast matrix operations are not available.

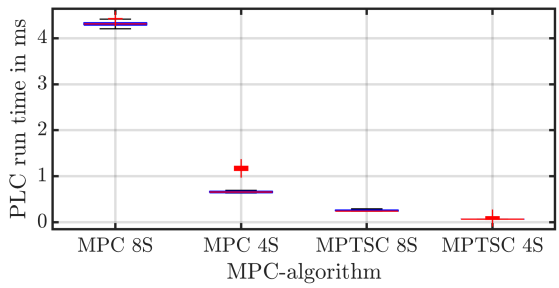

Fig. 8. PLC run time comparison of MPC and MPTSC with 4 and 8 states(S)

	runtime for PLC cycle	
	mean	σ
MPC with 8 States	4310.6 µs	36.3 µs
MPC with 4 States	660.0 µs	34.6 µs
MPTSC with 8 States	256.0 µs	16.5 µs
MPTSC with 4 States	73.2 µs	10.8 µs

TABLE II
COMPARISON OF RUNTIME OF MPC AND MPTSC.

To improve the control result, an additional load forecast can be used. The disturbance of the system, the load, can be predicted by an autoregressive or autoregressive integrated moving average (ARIMA) model. This forecast can then be used instead of the dead-time afflicted power measurement.

VII. CONCLUSION

In this paper, a new three-layer MPC cascade was presented for the application in industrial DC microgrids. By this extension, uncertainties in the industrial environment, which are caused by dynamic loads, can be considered consequently. As a proof of concept, the scheme for the new layer was presented in this paper and tested in an experimental setup. Since the standard MPC will be too slow for larger networks, a runtime comparison with a simpler MPTSC was performed. The results show that, especially without a parameter identified model, the proposed control scheme has equal control quality with faster runtimes. In the future, this approach will be used for stochastic control at any level.

REFERENCES

[1] M. Pellicciari, A. Avotins, K. Bengtsson, G. Berselli, N. Bey, B. Lennartsson, and D. Meike, "Areus—innovative hardware and software for sustainable industrial robotics," in *2015 IEEE International Conference on Automation Science and Engineering (CASE)*, pp. 1325–1332.
[2] F. Garcia-Torres and C. Bordons, "Optimal Economical Schedule of Hydrogen-Based Microgrids With Hybrid Storage Using Model Predictive Control," *IEEE Transactions on Industrial Electronics*, vol. 62, no. 8, pp. 5195–5207, 2015.
[3] J. M. Guerrero, J. C. Vasquez, J. Matas, L. G. de Vicuna, and M. Castilla, "Hierarchical Control of Droop-Controlled AC and DC Microgrids—A General Approach Toward Standardization," *IEEE Transactions on Industrial Electronics*, vol. 58, no. 1, pp. 158–172, 2011.
[4] J. Hu, Y. Shan, J. M. Guerrero, A. Ioinovici, K. W. Chan, and J. Rodriguez, "Model P redictive Control of Microgrids–An Overview," *Renewable and Sustainable Energy Reviews*, vol. 136, p. 110422, 2021.
[5] G. Bruni, S. Cordiner, V. Mulone, V. Sinisi, and F. Spagnolo, "Energy Management in a Domestic Microgrid by Means of Model Predictive Ccontrollers," *Energy*, vol. 108, pp. 119–131, 2016.
[6] C. A. Hans, P. Sopasakis, A. Bemporad, J. Raisch, and C. Reincke-Collon, "Scenario-based Model Predictive Operation Control of Islanded Microgrids," in *2015 54th IEEE Conference on Decision and Control (CDC)*, pp. 3272–3277.
[7] C. Bordons, F. Garcia-Torres, and M. A. Ridao, *Model Predictive Control of Microgrids*. Springer, 2020, vol. 358.
[8] S. Raimondi Cominesi, M. Farina, L. Giulioni, B. Picasso, and R. Scattolini, "A Two-Layer Stochastic Model Predictive Control Scheme for Microgrids," *IEEE Transactions on Control Systems Technology*, vol. 26, no. 1, pp. 1–13, 2018.
[9] S. Vazquez, J. Rodriguez, M. Rivera, L. G. Franquelo, and M. Norambuena, "Model Predictive Control for Power Converters and Drives: Advances and Trends," *IEEE Transactions on Industrial Electronics*, vol. 64, no. 2, pp. 935–947, 2017.
[10] T. Dragičević, "Model Predictive Control of Power Converters for Robust and Fast Operation of AC Microgrids," *IEEE Transactions on Power Electronics*, vol. 33, no. 7, pp. 6304–6317, 2018.
[11] A. Makarow, M. Keller, C. Rösmann, T. Bertram, G. Schoppel, and I. Glowatzky, *Model Predictive Trajectory Set Control for a Proportional Directional Control Valve*, Piscataway, NJ, 2017.
[12] K. M. Paasch, C. Cornaro, and M. Pierro, "PV-Grid Performance under Dynamic Weather Conditions," in *2019 IEEE Third International Conference on DC Microgrids (ICDCM)*, 2019, pp. 1–5.
[13] Gangui Yan, Dongyuan Liu, Junhui Li, and Gang Mu, "A Cost Accounting Method of the Li-ion Battery Energy Storage System for Frequency Regulation considering the effect of life degradation," *Protection and Control of Modern Power Systems*, vol. 3, no. 1, pp. 1–9, 2018.
[14] Leoni AG, "Technical Information - Medium Voltage Cable," 2021, accessed Jun. 28, 2018. [Online]. Available: https://publications.leoni.com/fileadmin/
[15] Bosch Rexroth AG, "Rexroth IndraDrive ML Universal Inverters HMU05: Instruction Manual," 2017, accessed Jun. 28, 2018. [Online]. Available: http://www.boschrexroth.com/various/utilities/mediadirectory
[16] M. S. Mahmoud, *Microgrid: Advanced Control Methods and Renewable Energy System Integration*. Elsevier, 2016.
[17] J. B. Rawlings, D. Q. Mayne, and M. Diehl, *Model Predictive Control: Theory, Computation, and Design*. Nob Hill Publishing Madison, WI, 2017, vol. 2.
[18] A. Männel, S. Tappe, E. Knöchelmann, and T. Ortmaier, "Investigation on an AC Grid Failure Handling of Industrial DC Microgrids with an Energy Storage," in *2019 IEEE International Conference on Industrial Technology (ICIT)*. IEEE, 2019, pp. 1710–1716.